Wind and Structures, Vol. 16, No. 1 (2013) 47-60
DOI: http://dx.doi.org/10.12989/was.2013.16.1.047

Internal pressures in buildings with a dominant opening and background porosity

P.Y. Kim * and J.D. Ginger

School of Engineering and Physical Sciences, James Cook University, Townsville, Queensland, Australia

(Received December 18, 2011, Revised April 11, 2012, Accepted April 13, 2012)

Abstract. A dominant opening in a windward wall, which generates large internal pressures in a building, is a critical structural design criterion. The internal pressure fluctuations are a function of the dominant opening area size, internal volume size and external pressure at the opening. In addition, many buildings have background leakage, which can attenuate internal pressure fluctuations. This study examines internal pressure in buildings for a range of dominant opening areas, internal volume sizes and background porosities. The effects of background porosity are incorporated into the governing equation. The ratio of the background leakage area A_L to dominant opening area A_W is presented in a non-dimensional format through a parameter, $\phi_6 - A_L / A_W$. Background porosity was found to attenuate the internal pressure fluctuations when ϕ_6 is larger than 0.2. The dominant opening discharge coefficient, k was estimated to lie between 0.05 to 0.40 and the effective background porosity discharge coefficient k'_L , was estimated to be between 0.05 to 0.50.

Keywords: background porosity; internal pressure; discharge coefficient; Helmholtz resonance; dominant opening; building

1. Introduction

The internal pressure in a building is dependent on the external pressure distribution, and the size and location of openings in the envelope. The pressure inside a nominally sealed building is generally smaller than the external pressure. However, the failure of a window or door can create a dominant windward wall opening and produce larger internal pressures; a critical design criterion.

The continuity of flow in and out of a building was used as the basis for specifying the mean internal pressure in a building by Liu (1975) and adopted in standards such as AS/NZS 1170.2 (2011). The fluctuating internal pressure in a building with a dominant opening was first studied by Holmes (1979) using the concept of the Helmholtz resonator. Further studies on model scale buildings with a dominant opening were carried out by Liu and Saathoff (1981), Liu and Rhee (1986), Stathopoulos and Luchien (1989) and Sharma and Richards (1997). The effects of sizes of dominant opening areas and volume on internal pressure were studied by Ginger et. al. (2008, 2010). Envelope flexibility has been considered by using an effective volume of the building as described by Vickery (1986). Ginger (2000) and Guha et. al. (2011a) have compared

∗Corresponding author, E-mail: peter.kim@my.jcu.edu.au

internal pressures measured in full scale buildings with analytical models. Guha *et al.* (2011b) incorporated flexibility and porosity explicitly in the analytical equations.

Vickery (1986, 1994) and Vickery and Bloxham (1992) studied the influence of background envelope porosity on internal pressure. They showed that porous openings exceeding nominally 10% of the dominant opening will attenuate the internal pressure fluctuations and porous openings larger than nominally 30% of the dominant opening will affect the mean internal pressure. Woods and Blackmore (1995) and Yu *et al.* (2008) also studied internal pressures in buildings with porosity and varying dominant opening areas and found that as the ratio of the leakage area to dominant opening area increases, the mean internal pressure is reduced. Oh (2007) developed a numerical model that treated each porous opening individually, using the power law equation, suggested by Shaw (1981). The power law assumes that the flow through porous openings is similar to flow in a pipe.

In the work described in this paper, internal pressure in a building with a range of volumes and windward wall openings with varying background porosities were studied using wind tunnel model tests and analytical methods. The variation of mean, fluctuations and peak internal pressures are presented in non-dimensional format that can be incorporated in building codes or design standards.

2. Internal pressure

The flow through an opening in a building can be described using the discharge equation shown in Eq. (1). Here, p_e is the external pressure at the opening and p_i is the internal pressure in the building, ρ is the density of air, U and $\dot{U}$ are the area averaged flow velocity and acceleration through the opening, respectively. The first term on the right side of the equation characterizes the losses and the second term is the inertial term describing a "slug" of air passing through the opening. The loss coefficient C_L can be represented as $1/k^2$, where k is the discharge coefficient and l_e is the effective length of the slug of air.

$$p_e - p_i = \frac{1}{2}\rho C_L U^2 + \rho l_e \dot{U} \tag{1}$$

Vickery and Bloxham (1992), noted that C_L and l_e can only be defined for situations such as steady flow through sharp edged circular openings connecting large volumes, where potential flow theory gives C_L = 2.68 (k=0.6) and $l_e = C_I\sqrt{A}$. Here, A is the opening area, and the inertial coefficient C_I, is $\sqrt{\pi/4}$ = 0.89. However, since potential flow conditions do not apply to highly turbulent flow through a building opening, experimental data must be used to estimate values for k and C_I. Previous studies have suggested a range of values for k from 0.15 to 1.0 and C_I of up to 2.

The pressure on the building $p(t)$, varying with time t, is expressed as a pressure coefficient, $C_p(t) = p(t)/\frac{1}{2}\rho\overline{U}_h^2$, where $\overline{U}_h$ is the mean wind speed at a height h. The statistical characteristics of the time varying pressure are presented as the mean $\overline{C}_p$, standard deviation

$C_{\sigma p}$ and maximum $\hat{C}_p$.

The principle of conservation of mass is combined with Eq. (1) to give the mean internal pressure in a building with windward and leeward opening areas, A_W and A_L respectively, as shown in Eq. (2).

$$\overline{C}_{pi} = \frac{\overline{C}_{pW}}{1+\left(\frac{A_L}{A_W}\right)^2} + \frac{\overline{C}_{pL}}{1+\left(\frac{A_W}{A_L}\right)^2} \tag{2}$$

Here, $\overline{C}_{pi}$ is the mean internal pressure in the building and $\overline{C}_{pW}$ and $\overline{C}_{pL}$ are the mean external pressure coefficients at the windward and leeward openings respectively.

Holmes (1979) and Vickery (1986) showed that the internal pressure fluctuations in a building with a dominant windward opening area A_W, are generated by a "slug" of air moving in and out of the opening and can be described by Eq. (3). Here, V_e is the effective internal volume, and a_s is the speed of sound. The undamped Helmholtz frequency is $f_H = \frac{1}{2\pi}\sqrt{a_s^2 A_W / l_e V_e}$.

$$\frac{l_e V_e}{a_s^2 A_W}\ddot{C}_{pi} + \left(\frac{V_e \overline{U}_h}{2a_s^2 k A_W}\right)^2 \dot{C}_{pi}\left|\dot{C}_{pi}\right| + C_{pi} = C_{pW} \tag{3}$$

Using dimensional analysis, Holmes (1979) represented Eq. (3) in terms of five non-dimensional parameters

$$\phi_1 = \frac{A_W^{3/2}}{V_e} \qquad \phi_2 = \frac{a_s}{\overline{U}_h} \qquad \phi_3 = \frac{\rho \overline{U}_h \sqrt{A_W}}{\mu} \qquad \phi_4 = \frac{\sigma_u}{\overline{U}} \qquad \phi_5 = \frac{\lambda_u}{\sqrt{A_W}}$$

where μ is viscosity of air and λ_u is the integral length scale of turbulence. By including a dimensionless time parameter $t^* = t\overline{U}_h / \lambda_u$, Eq. (3) can be expressed in non-dimensional format, Eq. (4).

$$\frac{C_I}{\phi_1 \phi_2^2 \phi_5^2}\frac{d^2 C_{pi}}{dt^{*2}} + \frac{1}{4k^2}\left(\frac{1}{\phi_1 \phi_2^2 \phi_5}\right)^2 \frac{dC_{pi}}{dt^*}\left|\frac{dC_{pi}}{dt^*}\right| + C_{pi} = C_{pW} \tag{4}$$

The $\phi_1 \phi_2^2$ parameters in the first and second terms of Eq. (4) can be replaced by the non-dimensional parameter $S^* = (A_W^{3/2} / V_e) \times (a_s / \overline{U}_h)^2$ as shown by Ginger *et al.* (2008, 2010). Eq. (5) shows the governing equation in non-dimensional S^* format. This implies that internal pressure fluctuations depend on the size of the opening area with respect to the size of the internal volume, and that there is a unique solution for C_{pi} for a given S^* and ϕ_S , if k and C_I are known.

$$\frac{C_I}{S^*\phi_5^2}\frac{d^2C_{pi}}{dt^{*2}}+\left(\frac{1}{4k^2}\right)\left(\frac{1}{S^*\phi_5}\right)^2\frac{dC_{pi}}{dt^*}\left|\frac{dC_{pi}}{dt^*}\right|+C_{pi}=C_{pW} \tag{5}$$

2.1 Background porosity

The previous section described the internal pressure response of a sealed building (no background porosity) with a dominant opening, however buildings will have varying degrees of background porosity. The background porosity in a building is generally difficult to quantify, and it is reasonable to assume a single effective lumped leakage area (Vickery and Bloxham 1992). Vickery (1986) showed that the inertial term for porous openings is orders of magnitude smaller than the damping term and can be ignored. Yu *et al.* (2008) and Guha *et al.* (2009) produced detailed derivations incorporating a lumped porous leeward opening area in the governing equation.

Ignoring the inertial term in Eq. (1), the air flow through an effective porous opening can be shown as $p_i - \overline{p}_L = \frac{1}{2}\rho C'_L U^2$, where $\overline{p}_L$ is the mean pressure acting on the leeward (i.e., porous) surfaces, and C'_L is the effective loss coefficient for the lumped porous opening and can be related to an effective discharge coefficient k'_L, by $C'_L = (1/\ k'_L)^2$. The parameter, *n*, is equal to the ratio of specific heats (1.4) for an adiabatic process. Using the continuity equation, the velocity, U, and the acceleration, $\dot{U}$ through the dominant opening can be found by Eqs. (6) and (7) respectively.

$$U=\frac{1}{2}\frac{\rho\overline{U}_h^2}{np_i}\frac{V_e}{A_W}\dot{C}_{pi}+\frac{A_L}{A_W}U_L \tag{6}$$

$$\dot{U}=\frac{1}{2}\frac{\rho\overline{U}_h^2}{np_i}\frac{V_e}{A_W}\ddot{C}_{pi}+\frac{A_L}{A_W}\dot{U}_L \tag{7}$$

U_L and $\dot{U}_L$ are the velocity and acceleration through the lumped leeward opening respectively, which are derived from the Bernoulli Equation. U_L and $\dot{U}_L$ are represented by

$$U_L=\overline{U}_h\sqrt{\frac{(C_{pi}-\overline{C}_{\rho L)}}{C'_L}} \qquad \dot{U}_L=\frac{\overline{U}_h\dot{C}_{pi}}{\left(2\times\sqrt{(C_{pi}-\overline{C}_{pL})C'_L}\right)}$$

The internal pressure fluctuations in a building, with a dominant windward opening and lumped leeward opening, are obtained by combining Eqs. (6), (7) and (3), to give Eq. (8) . It should be noted that a sealed building case (when A_L =0), gives Eq. (3).

$$\frac{l_eV_e}{a_s^2A_W}\ddot{C}_{pi}+\frac{k'_Ll_eA_L}{\overline{U}_hA_W}\cdot\frac{\dot{C}_{pi}}{\sqrt{(C_{pi}-\overline{C}_{pL})}}+\frac{\rho^2\overline{U}_h^2V_e^2}{4k^2n^2p_i^2A_W^2}\cdot\left(\frac{2k'_LA_Lnp_i}{V_e\rho\overline{U}_h}\cdot\sqrt{(C_{pi}-\overline{C}_{pL})}+\dot{C}_{pi}\right) \tag{8}$$

$$\cdot\left|\frac{2k'_L A_L np_i}{V_e \rho \bar{U}_h} \cdot \sqrt{(C_{pi} - \bar{C}_{pL})} + \dot{C}_{pi}\right| + C_{pi} = C_{pW}$$

The magnitude of background porosity in the building can be expressed by a non-dimensional parameter $\phi_6 = A_L / A_W$. Eq. (8) can then be represented in non-dimensional format shown in Eq. (9).

$$\frac{C_I}{S^*\phi_5^2}\frac{d^2C_{pi}}{dt^{*2}} + k'_L\frac{\phi_6}{\phi_5}\frac{C_I}{\sqrt{(C_{pi} - \bar{C}_{pL})}}\frac{dC_{pi}}{dt^*} + \frac{k_L'^2}{k^2}\phi_6^2(C_{pi} - \bar{C}_{pL}) + \frac{k'_L}{k^2}\frac{\phi_6}{S^*\phi_s}\sqrt{C_{pi} - \bar{C}_{pL}}\frac{dC_{pi}}{dt^*} + \left(\frac{1}{4k^2}\right)\left(\frac{1}{S^*\phi_s}\right)^2\frac{dC_{pi}}{dt^*}\left|\frac{dC_{pi}}{dt^*}\right| + C_{pi} = C_{pW} \quad (9)$$

3. Experimental and numerical methods

A series of model scale tests were carried out on a 400 mm × 200 mm × 100 mm building, in the wind tunnel at the School of Engineering and Physical Sciences at James Cook University. The model was extended 600 mm below the wind tunnel floor to allow the varying of internal volume by 3, 5 and 7 times the normal volume of the building shown in Fig. 1(a). Fig. 1(b) shows the layout of the building porosity. Background porosities *P1*, *P2*, *P3* and *P4* were modelled with 64 × 1.5 mm diameter holes and 54 × 3 mm diameter holes installed uniformly on the two side walls, the leeward wall and the roof, which could be blocked or opened as needed.
The windward external pressure coefficients C_{pW} , were measured on 30 taps across a door centred on the 400mm windward wall. The pressures were area averaged for four dominant opening areas: *A1* (20mm × 20mm), *A2* (25mm × 50mm), *A3* (50mm × 50mm) and *A4* (80mm × 50mm), shown in Fig. 1(c). The leeward pressure C_{pL} was obtained by area averaging pressures measured on the roof, side walls and leeward wall.

The internal pressure C_{pi} was measured in the model for each combination of windward wall opening areas: *A1, A2, A3, A4*, volumes: *V3, V5, V7* and background porosities: *P1, P2, P3, P4* given in Table 1. Each windward opening area, porosity and volume gives a set of S^*, ϕ_5 and ϕ_6 values.

Generally all of the non-dimensional parameters cannot be matched between full scale and model scale as needed for similarity requirements. The effects of Reynolds number mismatch are not explicitly accounted for in this study. This is assumed to have a negligible effect for the dominant opening sizes considered here, but may influence the discharge coefficients for the background porosity. The results herein provide a general trend of the effects of background porosity.

The atmospheric boundary layer was scaled at 1/200 for Terrain Category 2 as defined by AS/NZS 1170.2 (2011). Tests were conducted at a mean approach wind speed of approximately 10 m/s at roof height, $\bar{U}_h$ (height = 100 mm model scale). The integral length scale of turbulence λ_u at roof height was estimated to be 300 mm. Pressures were sampled at 1250 Hz for 30 seconds using dynamic pressure measurement system from Turbulent Flow Instrumentation. The experimental setup is similar to that described by Ginger *et al*. (2010).

The numerical model described by Ginger *et al*. (2008, 2010) was used to simulate internal pressure time histories for the range of volume and dominant opening sizes with varying porosity. The measured external pressures at the dominant opening were used to solve Eq. (8) by a first order explicit finite difference scheme

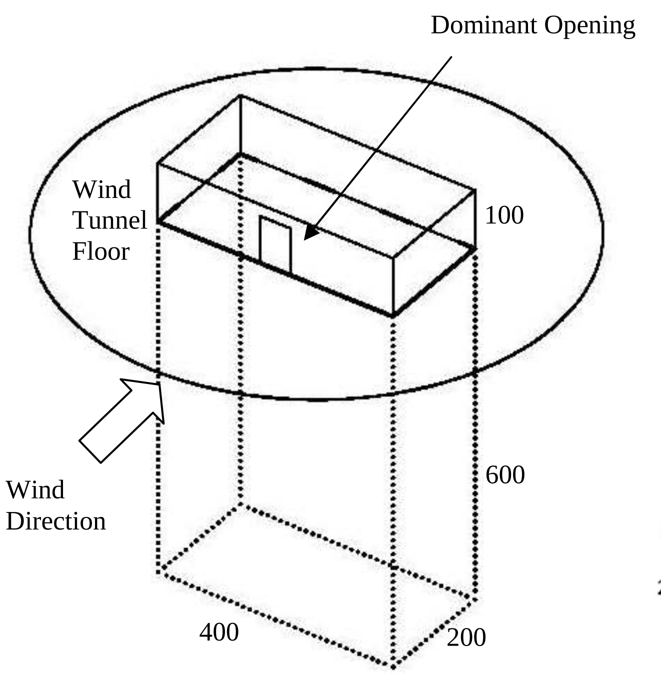

(a) Wind tunnel model with 600mm extension below the floor

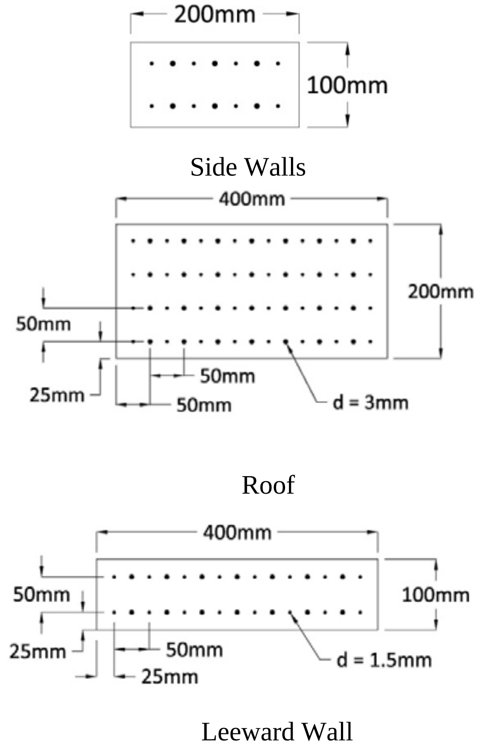

(b) Simulated porosity on leeward surfaces

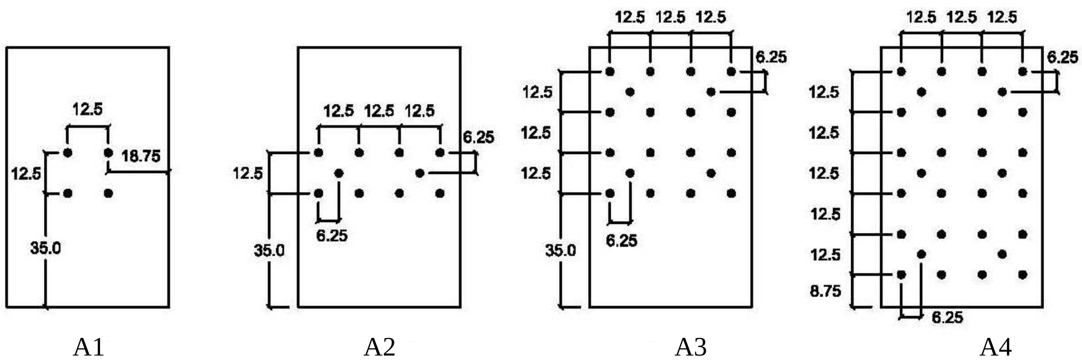

(c) Varying opening area and external pressure taps used to windward wall pressures (dimensions in mm)

Fig. 1 200 mm x 400 mm x 100 mm wind tunnel model

Table 1 Test configurations opening size, volume size, S^*, leakage area A_L with corresponding ϕ_5 , and ϕ_6

A_W (mm^2)	Volume (mm^3)	S^*	A_L (mm^2)	ϕ_6
$A1$ = 20×20, ϕ_5 = 15.0	$V3$ = 200×400×300	0.46	P1 = 0	0
			P2 = 113	0.28
			P3 = 382	0.95
			P4 = 495	1.24
	$V5$ = 200×400×500	0.25	P1 = 0	0
			P2 = 113	0.28
			P3 = 382	0.95
			P4 = 495	1.24
	$V7$ = 200×400×700	0.17	P1 = 0	0
			P2 = 113	0.28
			P3 = 382	0.95
			P4 = 495	1.24
$A2$ = 50×25, ϕ_5 = 8.5	$V3$ = 200×400×300	2.56	P1 = 0	0
			P2 = 113	0.09
			P3 = 382	0.31
			P4 = 495	0.40
	$V5$ = 200×400×500	1.38	P1 = 0	0
			P2 = 113	0.09
			P3 = 382	0.31
			P4 = 495	0.40
	$V7$ = 200×400×700	0.95	P1 = 0	0
			P2 = 113	0.09
			P3 = 382	0.31
			P4 = 495	0.40
$A3$ = 50×50, ϕ_5 = 6.0	$V3$ = 200×400×300	7.24	P1 = 0	0
			P2 = 113	0.05
			P3 = 382	0.15
			P4 = 495	0.20
	$V5$ = 200×400×500	3.90	P1 = 0	0
			P2 = 113	0.05
			P3 = 382	0.15
			P4 = 495	0.20
	$V7$ = 200×400×700	2.69	P1 = 0	0
			P2 = 113	0.05
			P3 = 382	0.15
			P4 = 495	0.20
$A4$ = 80×50, ϕ_5 = 4.7	$V3$ = 200×400×300	14.65	P1 = 0	0
			P2 = 113	0.03
			P3 = 382	0.09
			P4 = 495	0.12
	$V5$ = 200×400×500	7.90	P1 = 0	0
			P2 = 113	0.03
			P3 = 382	0.09
			P4 = 495	0.12
	$V7$ = 200×400×700	5.44	P1 = 0	0
			P2 = 113	0.03
			P3 = 382	0.09
			P4 = 495	0.12

4. Results and discussions

The mean, standard deviation and maximum internal and external pressures were measured for each test configuration described in Table 1. The mean external pressure on the windward and leeward surfaces was used to predict the mean internal pressure using Eq. (2). Fig. 2 compares the measured and theoretical $\overline{C}_{pi}$ to $\overline{C}_{pW}$ ratios from Eq.(2), with varying effective leeward openings, ϕ_6. The theoretical results show that when ϕ_6 is less than approximately 0.2, $\overline{C}_{pi}$ is within 10% of $\overline{C}_{pW}$. However, when ϕ_6 is larger than 0.2, the mean internal pressures are significantly reduced in comparison with the external pressures at the windward opening. The measured mean pressures follow the same trends and are similar to those obtained by Vickery (1994).

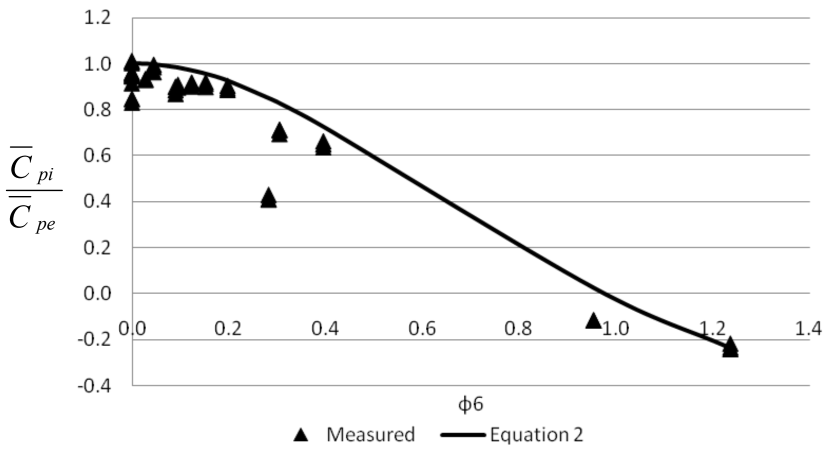

Fig. 2 Ratio of internal and external mean pressure coefficients to ϕ_6

The ratio of the measured $C_{\sigma pi}$ to $C_{\sigma pW}$ versus S^* are presented for ranges of ϕ_6 in Fig. 3. When ϕ_6 is less than 0.1, the internal pressure fluctuations were greater than the external pressure fluctuations for S^* values larger than 0.5. For cases when S^* is less than 0.5, the internal pressure fluctuations are greatly reduced compared to external pressure fluctuations. This figure also shows that when the background porosity is increased the internal pressure fluctuations are attenuated. The magnitude of the reduction is dependent on the magnitude of the porous area to dominant opening area, ϕ_6. For low ϕ_6 values between 0.1 and 0.2, the attenuation of the internal pressure fluctuation is small. However, when ϕ_6 is greater than 0.2 the internal pressure fluctuations decrease by greater than 20%, especially when S^* is less than 0.5. The ratio of the measured $\hat{C}_{pi}$ to $\hat{C}_{pW}$ is shown in Fig. 4. The measured peak pressures follow similar trends to the measured standard deviations. The results for the sealed building case are similar to those found by Ginger *et al.* (2010).

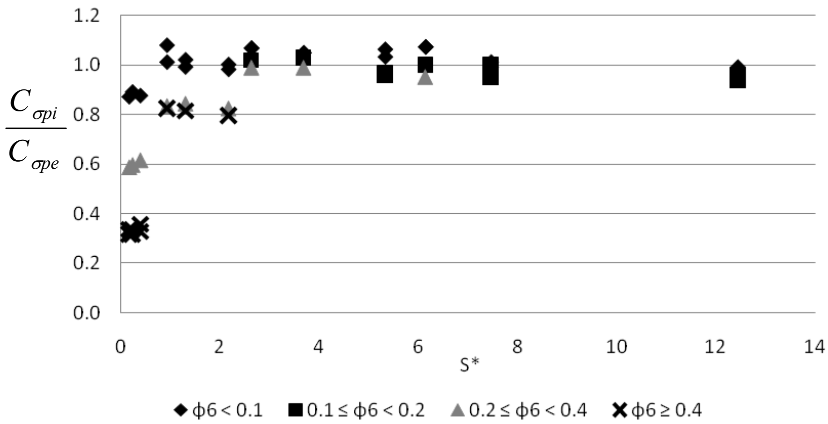

Fig. 3 Ratio of internal and external pressure standard deviation versus S^* for varying ϕ_6

The measured external and internal pressure spectra, $S_{Cp}(f)$, with varying background porosities *P1*, *P2*, *P3* and *P4*, for opening area *A2* with volumes *V3* and *V7,* are shown in Figs. 5 (a) and (b), and opening area *A4* with volumes *V3* and *V7*, are shown Fig. 6 (a) and (b). When the building is sealed (*P1*), Figs. 5 (a) and (b) show a distinct Helmholtz resonance at approximately 45 Hz and 40 Hz respectively. In both cases, increasing the porosity from *P2, P3* to *P4* progressively reduces the magnitude of the Helmholtz peak. This increased damping is caused by large values of ϕ_6 in the second and third terms of Eq. (9). For this case ϕ_6 was equal to 0.09, 0.31 and 0.40 for porosities *P2*, *P3* and *P4* respectively. When ϕ_6 is equal to 0.31 and 0.40, the Helmholtz resonance is almost completely damped. Similar trends are observed in Figs. 6 (a) and (b), however there is less attenuation of the Helmholtz peaks due to smaller ϕ_6 values. The ϕ_6 values in Figs. 6(a) and (b) were 0.03, 0.09 and 0.12 for *P2*, *P3* and *P4* respectively.

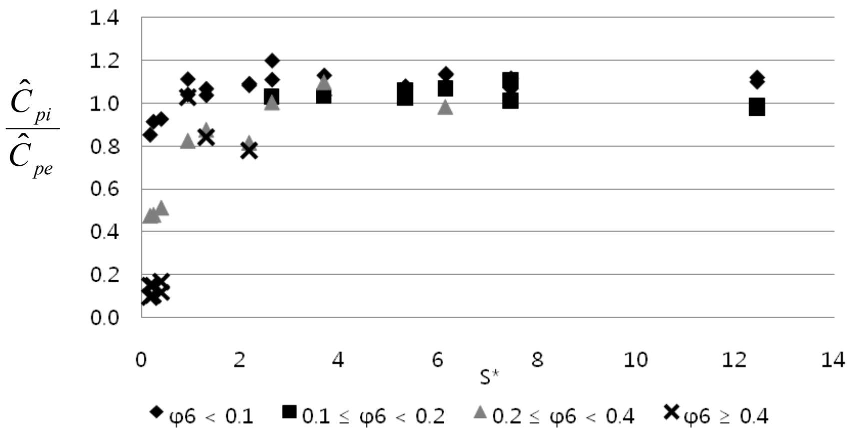

Fig. 4 Ratio of internal and external peak pressure coefficient versus S^* for varying ϕ_6

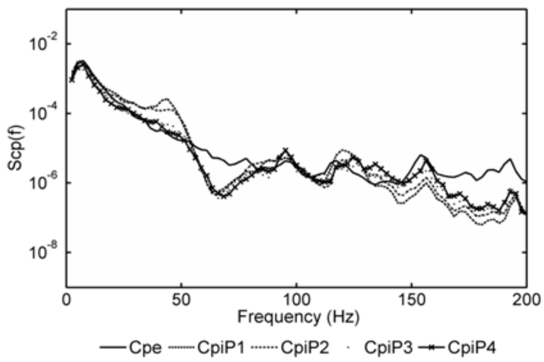

(a) Opening area *A2* and volume *V3*

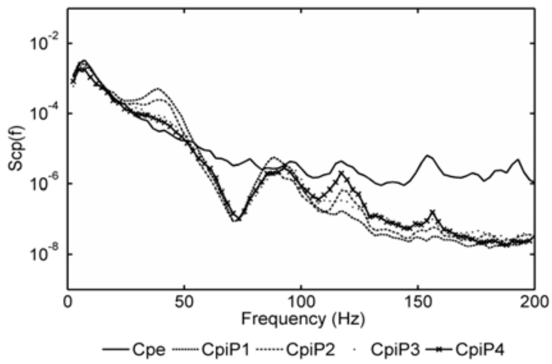

(b) Opening area *A2* and volume *V7*

Fig. 5 Measured external and internal pressure spectra for varying porosities *P1*, *P2*, *P3* and *P4* for area *A2* and volumes *V3* and *V7*

Simulated internal pressure spectra generated from the numerical model were matched with measured internal pressure spectra obtained from the wind tunnel results by varying the parameters: C_I, k and k'_L. The inertial coefficient C_I was estimated to be about 2.0 by matching the Helmholtz frequencies. Vickery (1994) also stated that C_I could be up to a value of 2 for highly fluctuating flow. Guha *et al.* (2009) and Sharma and Richards (1997) used a separate flow coefficient to account for the contraction of the air slug at the opening that gives an overall equivalent C_I of approximately 1.5. The windward wall opening discharge coefficient k , was estimated using the sealed building case (*P1*) and matching the magnitude of the Helmholtz resonance peak. k was assumed to remain constant for all porous cases. The background leakage discharge coefficient k'_L was adjusted to match internal pressure spectra for *P2*, *P3* and *P4*. The measured and simulated internal pressure spectra for configurations *A2-V7* and *A4-V7* with porosities of *P1, P2, P3* and *P4* are presented in Figs. 7 and 8 , respectively. The simulations show that the numerical model matches the measured wind tunnel results.

The estimated values of k range from 0.1 to 0.4 for various S^*, shown in Fig. 9. The discharge coefficient for the dominant opening, k, decreases when S^* increases. This suggests that when the opening area is small and the volume is large, the airflows through the orifice more freely, similar to flow through an orifice connecting two infinitely large volumes. Conversely when the opening area is large and the volume is small, the flow is impeded and results in a smaller discharge coefficient. Similar findings were published by Ginger *et al.* (2010). Recent experiments by Kim and Ginger (2012) showed that when air flow oscillates in and out of an orifice, the values of k can be reduced to within this range.

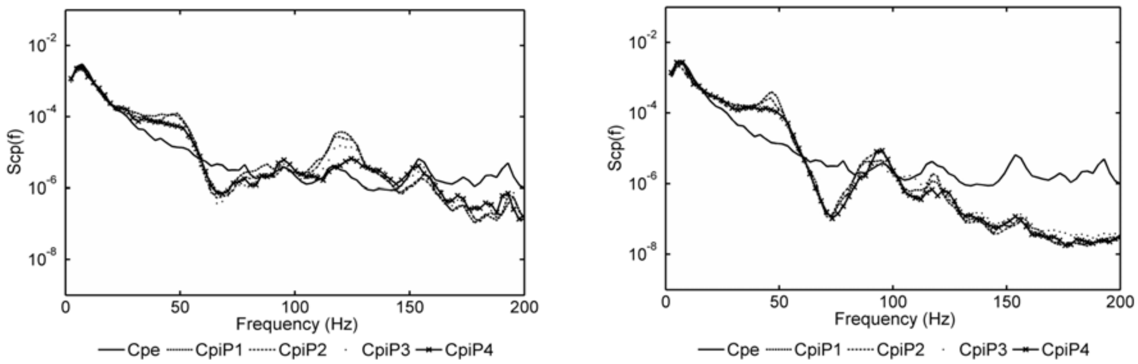

(a) Opening area *A4* and volume *V3* (b) Opening area *A4* and volume *V7*

Fig. 6 Measured external and internal pressure spectra for varying porosities *P*1, *P*2, *P*3 and *P*4 for area *A*4 and volumes *V*3 and *V*7

Fig. 10 shows the effective discharge coefficient k'_L for the background leakage area with increasing S^* and varying ϕ_6. The estimated values of k'_L have a large variation, ranging from 0.05 to 0.5. Fig. 10 shows that in general, for larger ϕ_6 values, the estimated k'_L values tend to decrease. This may be explained by the fact that the increase in porosity results in a reduction in internal pressure and a lower pressure drop across the leeward surfaces. This results in a small discharge coefficient.

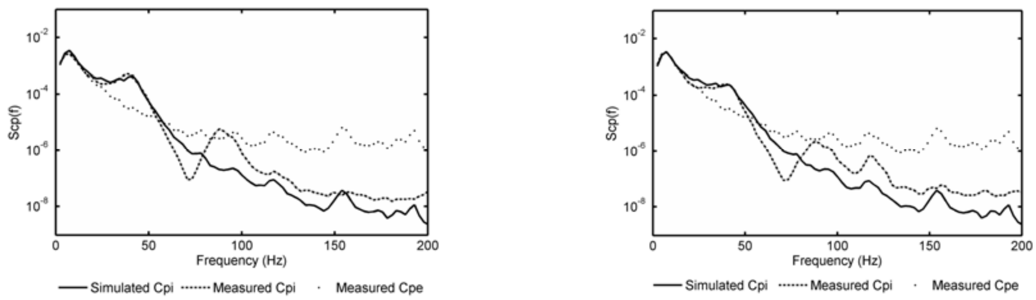

(a) Porosity *P1, k*= 0.35 (b) Porosity *P2, k*= 0.35 k'_L =0.4

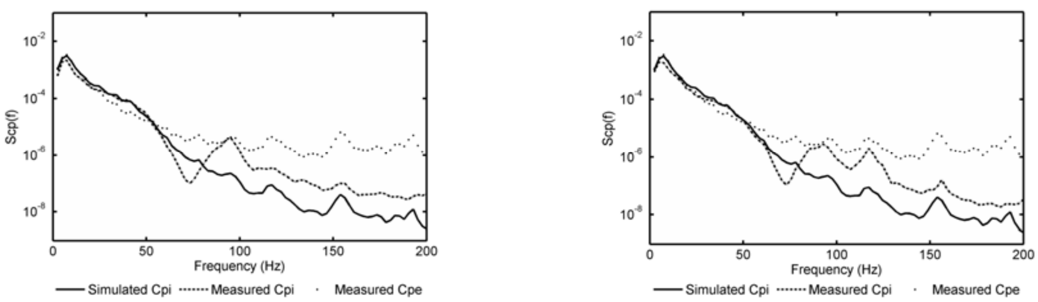

(c) Porosity *P3, k*= 0.35 k'_L = 0.25 (d) Porosity *P4, k*= 0.35 k'_L = 0.22

Fig. 7 Area *A2* and internal volume *V7* for porosities with opening *k* = 0.35 and varying k'_L

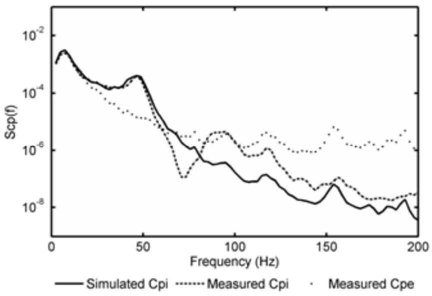

(a) Porosity *P1, k*= 0.15

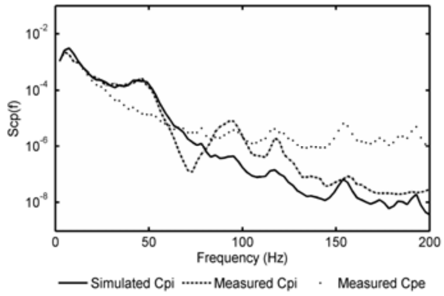

(b) Porosity *P2, k*= 0.15 k'_L =0.4

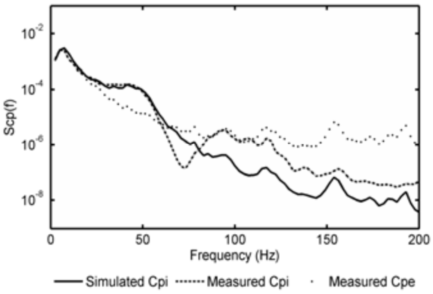

(c) Porosity *P3, k*= 0.15, k'_L =0.2

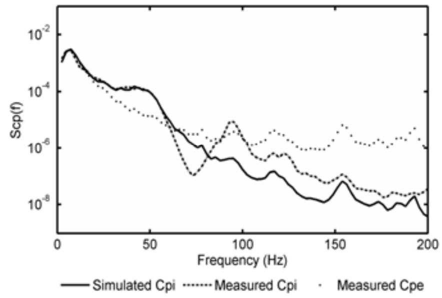

(c) Porosity *P4, k*= 0.15, k'_L =0.15

Fig. 8 Area *A4* and internal volume *V7* for porosities with opening k = 0.15 and varying k'_L

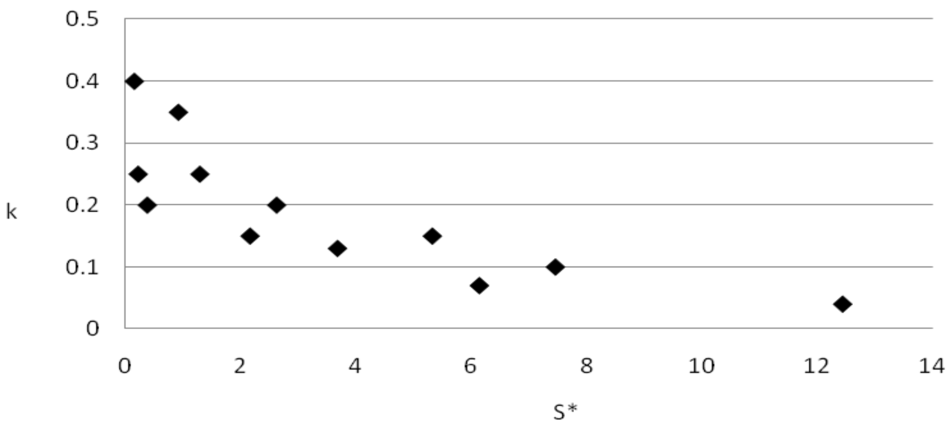

Fig. 9 Discharge coefficient for dominant opening *k* with increasing S^* for $\phi_6 = 0$

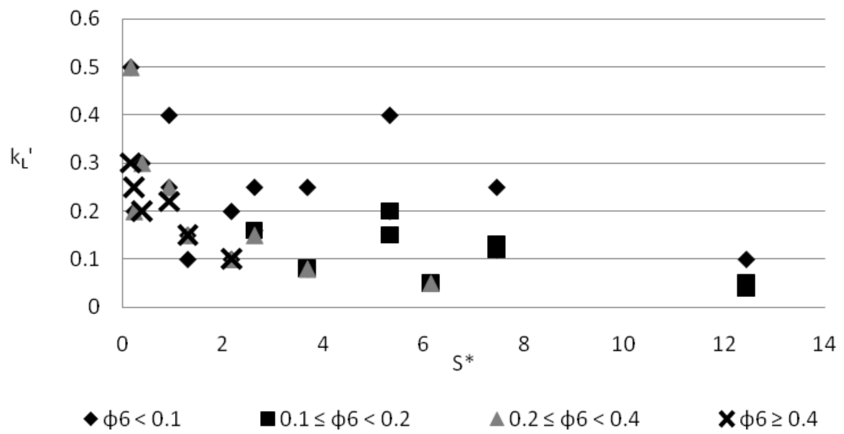

Fig. 10 Discharge coefficient for background porosity k'_L with increasing S^*

5. Conclusions

The effects of internal pressure fluctuations in buildings with a range of internal volumes, dominant opening areas and background porosities were studied using a combination of analytical methods and a series of wind tunnel model experiments. The mean, standard deviation and maximum internal pressures were compared to the corresponding external pressure at the windward dominant opening and presented using a series of non-dimensional parameters: the dominant opening area to volume parameter $S^* = (a_s / \overline{U}_h)^2 (A_W{}^{3/2} / V_e)$ and background porous area to dominant opening area parameter $\phi_6 = A_L / A_W$. The discharge coefficients for the dominant opening *k* and effective discharge coefficient for the lumped background porosity area k'_L were estimated by matching spectra. The study found that :

- The non-dimensional form of the governing equation for internal pressure can be modified to incorporate an effective lumped background leakage area by a dimensionless $\phi_6 = A_L / A_W$ parameter.
- For background porosity cases where ϕ_6 is less than 0.2, has is minimal affect on the $\overline{C}_{pi}$. However, when ϕ_6 is greater than 0.2, a reduction in $\overline{C}_{pi}$ greater than 10% can be expected.
- Internal pressure fluctuations are influenced by dominant opening size, internal volume size and amount of background porosity.
- $C_{\sigma pi}$ are attenuated by larger than 20% when ϕ_6 is larger than 0.2.
- The dominant opening discharge coefficient *k*, is dependent on the sizes of the opening area and internal volume.
- Discharge coefficients were estimated to be between 0.05 to 0.40. These values are lower than the theoretical value of 0.61 for potential flow. Similar trends were found by Ginger *et al*. (2010). The effective discharge coefficient of the lumped porous area k'_L was estimated to be in the range of 0.05 and 0.50.

- The inertial coefficient C_I, of 2 satisfactorily predicts the Helmholtz frequency.

References

Ginger, J.D. (2000), "Internal pressures and cladding net wind loads on full-scale low-rise building", *J. Struct. Eng.*- ASCE, **126**(4), 538-543.
Ginger, J.D., Holmes, J.D. and Kim, P.Y. (2010), "Variation of internal pressure with varying sizes of dominant openings and volumes", *J. Struct. Eng.*- ASCE, **136**(10), 1319-1326.
Ginger, J.D., Holmes, J.D. and Kopp, G.A. (2008), "Effect of building volume and opening size on fluctuating internal pressures" , *Wind Struct.*, **11**(5), 361-376.
Guha, T.K., Sharma, R.N. and Richards, P.J. (2011a), "Full-scale studies of wind induced internal pressure in a warehouse", *Proceedings of the 13th International Conference on Wind Engineering*, Amsterdam, Netherlands.
Guha, T.K., Sharma, R.N. and Richards, P.J. (2011b), "On the internal pressure dynamics of a leaky and flexible low rise building with a dominant opening", *Proceedings of the 13th International Conference on Wind Engineering*, Amsterdam, Netherlands.
Guha, T.K., Sharma, R.N. and Richards, P.J. (2009), "The effect of background leakage on wind induced internal pressure fluctuations in a low rise building with a dominant opening", *Proceedings of the 11th Americas Conference on Wind Engineering*, San Juan, Puerto Rico.
Holmes, J.D. (1979), "Mean and fluctuating internal pressure induced by wind", *Proceedings of the 5th International Conference on Wind Engineering*, Fort Collins, USA.
Kim, P.Y. and Ginger, J.D. (2012), "Discharge coefficients for a dominant opening in a building", *Proceedings of the 15th Australasian Wind Engineering Society Workshop*, Sydney, Australia.
Liu, H. (1975), "Wind pressure inside buildings" *Proceedings of the 3rd US National Conference on Wind Engineering*, Fort Collins, USA.
Liu, H. and Rhee, K.H. (1986), "Helmholtz oscillation in building models", *J. Wind Eng. Ind. Aerod.*, **24**(2), 95-115.
Liu, H and Saathoff, P. (1981), "Building internal pressure: sudden change", *J. Eng. Mech. Div.,* **107**(2), 309-321.
Oh, J.H., Kopp, G.A. and Inculet, D.R. (2007), "The UWO contributions to the NIST aerodynamic database for wind loads and low buildings Part 3: Internal pressures", *J. Wind Eng. Ind. Aerod.,* **95**(8), 755-779.
Sharma, R.N. and Richards, P.J. (1997), "The effect of roof flexibility on internal pressure fluctuations", *J. Wind Eng. Ind. Aerod.,* **72**, 175-186.
Shaw, C.Y. (1981), "Airtightness: supermarkets and shopping malls", *ASHRAE J.*, **23**, 44-46.
Standards Australia/Standards New Zealand (2011), *Structural design actions - Part 2: Wind actions*, – AS/NZS 1170.2:2011, Standards Australia International Ltd., Sydney, NSW, Australia and Standards New Zealand, Wellington, NZ.
Stathopoulos, T. and Luchian, H.D. (1989), "Transient wind induced internal pressures" *J. Eng. Mech.*- ASCE. **115** (7), 1501-1514.
Vickery, B.J. (1986), "Gust factors for internal pressures in low-rise buildings", *J. Wind Eng. Ind. Aerod.,* **23**, 259-271.
Vickery, B.J. (1994), "Internal pressures and interactions with the building envelope" *J. Wind Eng. Ind. Aerod.,* **53**(1-2), 125-144.
Vickery, B.J. and Bloxham, C. (1992), "Internal pressure dynamics with a dominant opening", *J. Wind Eng. Ind. Aerod.,* **41**(1-3), 193-204.
Woods, A.R. and Blackmore, P.A. (1995), "The effect of dominant openings and porosity on internal pressures", *J. Wind Eng. Ind. Aerod.,* **57**(2-3), 167-177.
Yu, S.C., Lou, W.J. and Sun, B.N. (2008), "Wind-induced internal pressure response for structure with single windward opening and background leakage" *J. Zhejiang University*, **9**(3), 313-321.